Journal of Science and Technology – Engineering and Technology for Sustainable Development
Volume 36, Issue 2, April 2026, 070–078

Modeling and Evaluation of the Regenerative Performance of an All-Wheel-Drive Electric Vehicle under Vietnamese Driving Conditions

Dao Thanh Tung, Tran Trong Dat, Nguyen Quoc Trieu, Dam Hoang Phuc*, Le Van Nghia, Duong Ngoc Khanh
Hanoi University of Science and Technology, Hanoi, Vietnam
**Corresponding author email: phuc.damhoang@hust.edu.vn*

Abstract

The study presents a comprehensive analysis of the regenerative braking efficiency of an All-wheels-drive electric vehicle under different traffic conditions using specific simulation software. The proposed model evaluates energy recovery performance across non-rush hours, rush hours, and highway driving cycles in Vietnam, highlighting the influence of traffic density on regenerative braking effectiveness. The results indicate that the highest energy recovery occurs in non-rush hours, where frequent braking events enhance regenerative braking activation. A comparative assessment between low and high-regeneration braking modes shows that the efficiency gap varies significantly depending on traffic flow, with the high-regeneration braking mode consistently demonstrating superior performance. In highway conditions, energy recovery is notably lower due to stable cruising speeds and fewer braking instances. The findings of this research contribute to the advancement of energy-efficient electric vehicle technologies by providing a detailed evaluation of regenerative braking potential under Vietnam driving conditions. This study serves as a reference for optimizing vehicle control strategies and promoting sustainable transportation solutions. By understanding the impact of traffic patterns on regenerative braking efficiency, this research aids in enhancing energy recovery strategies, reducing overall energy consumption, and improving vehicle performance in real-world urban environments.

Keywords: All-wheel-drive electric vehicle, braking force distribution, energy recovery, regenerative braking, simulation model, traffic conditions.

1. Introduction

With the increasing demand for sustainable transportation, electric vehicles (EVs) have become a focal point in the automotive industry. The regenerative braking system (RBS) plays a crucial role in enhancing energy efficiency by converting kinetic energy into electrical energy to recharge the battery. However, optimizing regenerative braking performance while maintaining vehicle stability remains a challenge, particularly under diverse driving conditions.

Numerous studies worldwide have explored regenerative braking and its control algorithms. Giulia Sandrini and co-authors [1] propose a regenerative braking logic that maximizes energy recovery while ensuring vehicle stability. Their model optimizes regenerative torque for front-, rear-, and all-wheel-drive (AWD) systems, preventing wheel lockup and integrating conventional braking when necessary. Energy recuperation is prioritized, followed by optimal braking force distribution, particularly in AWD vehicles managing dual-motor torque. Simulations on compact EVs demonstrate WLTC cycle energy savings of 29.5–30.3% over non-regenerative braking and 22.6–23.5% over conventional strategies. In the US06 cycle, energy consumption is reduced by 23.9–24.4% and 19.0–19.5%, respectively. Juan Valladolid and co-authors [2] analyze regenerative braking efficiency under real-world driving conditions and varying road topographies. Key influencing factors include vehicle mass, torque, speed, road inclination, and braking duration, while driving modes were excluded due to a standardized pace. The study integrates real-world energy regeneration data to enhance system optimization for automotive applications. State of charge (SOC), speed, torque, and terrain significantly impact braking efficiency, as irregular road conditions induce aggressive physical forces, reducing energy autonomy. Quantitative analysis yields experimental surfaces and curves, demonstrating 78% energy recovery despite the vehicle's limited range. Myeong Hwan Hwang and co-authors [3] propose a Comfort Regenerative Braking System (CRBS) utilizing artificial neural networks for braking control. Autonomous vehicle comfort is primarily governed by control algorithms, which can be optimized by predicting passenger comfort based on acceleration and deceleration thresholds. Numerical analysis ensures reduced jerk conditions, while backward propagation refines braking force estimation for enhanced accuracy. The algorithm was validated

p-ISSN 3093-3242
e-ISSN 3093-3579
https://doi.org/10.51316/jst.189.etsd.2026.36.2.9
Received: Mar 26, 2025; Revised: Aug 26, 2025
Accepted: Oct 2, 2025; Online: Mar 24, 2026.

through CarSim and MATLAB/Simulink simulations, demonstrating superior performance over conventional braking. The proposed CRBS optimizes regenerative braking while enhancing passenger comfort.

Although numerous studies have explored RBS and regenerative braking control algorithms, most of them focus on standardized driving conditions such as WLTP or US06, without fully considering the impact of traffic density, road surface conditions, and driver behavior in real-world environments. Previous studies often assume ideal conditions, where vehicles can maximize regenerative braking without being affected by unpredictable traffic variations. However, in high-density urban areas, electric vehicles frequently encounter sudden stop-and-go situations, uneven braking forces, and fluctuating traffic speeds. These factors directly affect the energy recovery efficiency of the RBS and may reduce the overall performance of the vehicle.

Therefore, this study not only evaluates the regenerative braking performance of AWD electric vehicles but also analyzes the effects of real-world factors such as different driving cycles (rush hours, non-rush hours, highway), road adhesion coefficients, and braking force distribution strategies. By utilizing experimental data collected from a VinFast VF8 operating on the streets of Vietnam, this research identifies the energy recovery efficiency under varying conditions. Based on these findings, the study proposes improvements in braking control strategies to optimize regenerative braking performance and enhance the driving experience in actual traffic environments.

2. Evaluation Method

2.1. Building a Simulation Model of the EV

The reference object in the article chosen is the VinFast VF8 with technical specifications as shown in table 1 below:

Table 1. Parameters of the reference vehicle [9]

Parameters	**Value**
Overall dimension	4750 x 1934 x 1667(mm)
Wheelbase	2950(mm)
Battery Capacity	87,7(kWh)
Charging speed	10% - 70% in 31 min
Max. power	260(kW)

The electric vehicle model is developed using several fundamental models, including the vehicle model, tire model, braking model (which encompasses both regenerative and mechanical braking), electric motor model, battery model, and driver model. This model of the AWD EV has been established in previous study which can be seen in authorized articles [6, 7]. The acceleration pedal model is represented by a signal ranging from -1 to 1, where -1 corresponds to full braking and 1 corresponds to full acceleration.

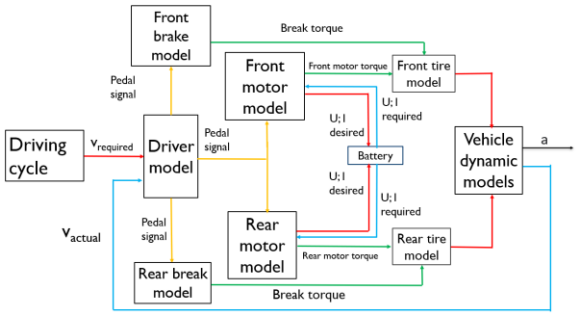

Fig. 1. EVs model

The simulation structure is based on an input driving cycle, where the driver model utilizes a PID controller to regulate throttle and brake pedal signals. The pedal signal is input into the braking model and motor model to determine the torque distribution between the front and rear axles. The total braking force, derived from both mechanical and regenerative braking, is distributed according to an optimized strategy to ensure energy recovery efficiency and vehicle stability. Additionally, the torque generated by the front and rear axles is fed into the battery model and electric motor model to determine the energy consumption required to meet the motor's torque demand. The vehicle dynamics model and wheel dynamics model are then used to calculate key dynamic parameters such as velocity, acceleration, and travel distance.

The model is validated by comparing simulation results with driving cycle WLTP and experimental data collected from dynamic sensors installed on a VinFast VF8 operating on real-world roads. Model accuracy is evaluated using the mean absolute error (MAE) and the root mean square error (RMSE). After validation, it is applied to analyze regenerative braking performance in Vietnam's driving cycles.

2.2. Developing a Regenerative Braking Control Algorithm Based on Theoretical Brake Force Distribution

2.2.1. Theoretical braking force distribution

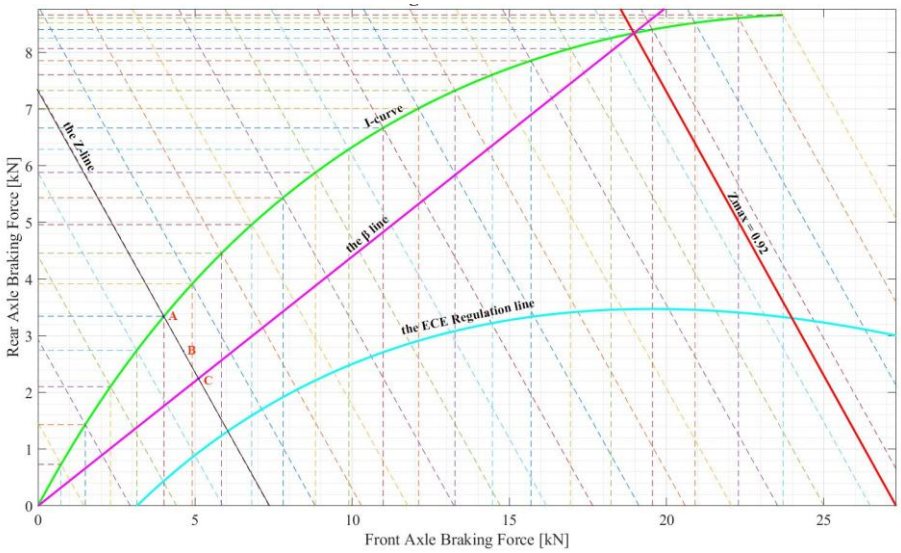

Fig. 2. Braking force distribution strategy based on curve I [4]

During braking, the vehicle achieves optimal braking performance when the braking forces at the wheels fully utilize the available traction, and the brake force distribution ratio between the axles matches the traction force ratio on the axles. The ideal braking force distribution scenario is illustrated in Fig. 2, where the optimal distribution of braking force between the front and rear wheels follows Curve I, as expressed by the following equation:

$$\frac{F_{\mu 1}}{F_{\mu 2}} = \frac{F_{z1}}{F_{z2}} = \frac{b + zh_g}{a - zh_g} \tag{1}$$

where $F_{\mu 1}$ and $F_{\mu 2}$ are the braking forces applied to the front and rear wheels, F_{z1} and F_{z2} are respectively the ground normal reaction force of the front wheel and rear wheel, a and b are respectively the longitudinal distance from the center of gravity to the front axle and rear axle, z is the braking strength, h_g is the height of the vehicle's center of gravity.

The braking strength z can be given as:

$$z = \frac{\dot{v}_d}{g} \tag{2}$$

where: $\dot{v}_d$ is the braking deceleration, g equal 9.8 m/s^2 is the acceleration of gravity.

The Z-line represents the total braking torque of both axles corresponding to different braking accelerations when distributing braking force. The β-line denotes the hydraulic braking force distribution between the front and rear axles. To achieve optimal braking efficiency, the objective of the braking force distribution strategy is to determine point A, which is the intersection of the Z-line and Curve I.

Thus, the control algorithm will focus on ensuring that the total regenerative and hydraulic braking torque does not exceed the required braking torque value defined by Curve I across different braking decelerations.

2.2.2. Control strategy

There are two common regenerative braking strategies: the series strategy and the parallel strategy, as illustrated in Fig. 3 below. In the parallel strategy, regenerative braking and mechanical braking are activated simultaneously, with regenerative braking operating until it reaches its maximum capacity. In the series strategy, regenerative braking is activated first, and mechanical braking is only engaged once regenerative braking reaches its maximum limit [8].

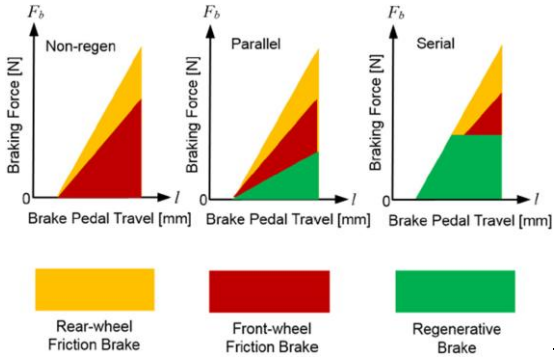

Fig. 3. Three different control strategies for regenerative braking [8]

The RBS in this study mainly works in normal braking conditions. Under normal braking, the focus is on maximizing energy recuperation while ensuring braking efficiency and stability. The braking force distribution strategy considers different adhesion coefficients and braking strengths to optimize energy recovery. As a result, the series regenerative braking strategy is chosen for the control algorithm.

The braking force of the front and rear axles is composed of hydraulic braking force and electric motor braking force, which can be expressed as [5]:

$$\begin{cases} F_{xb1} = F_{hy\_F} + F_{reg1} \\ F_{xb2} = F_{hy\_R} + F_{reg2} \\ F_Z = F_{xb1} + F_{xb2} \end{cases} \quad (3)$$

where: F_z is the total braking force of the front and rear axles, F_{xb1} and F_{xb2}, are respectively the total braking forces of the front axle and rear axle. F_{hy_F} and F_{hy_R} are respectively the hydraulic braking forces of the front axle and rear axle. F_{reg1} and F_{reg2} are respectively the electric motor braking forces of the front axle and rear axle.

To ensure braking stability, the braking torque of the front axle should first meet curve I as follows:

$$F_{FI} = F_{xb1} = F_{hy\_F} + F_{reg1} \quad (4)$$

where: F_{FI} is the theoretical braking force of the front axle.

The development of the regenerative braking control algorithm is divided into two main cases. The first case corresponds to the condition where the pedal signal is less than 0, indicating that the driver is actively applying the brake pedal. The second case corresponds to the condition where the pedal signal is 0, meaning the driver is not engaging with any pedals. The control algorithm logic of braking force distribution is proposed as shown in Fig. 4 and Fig. 5.

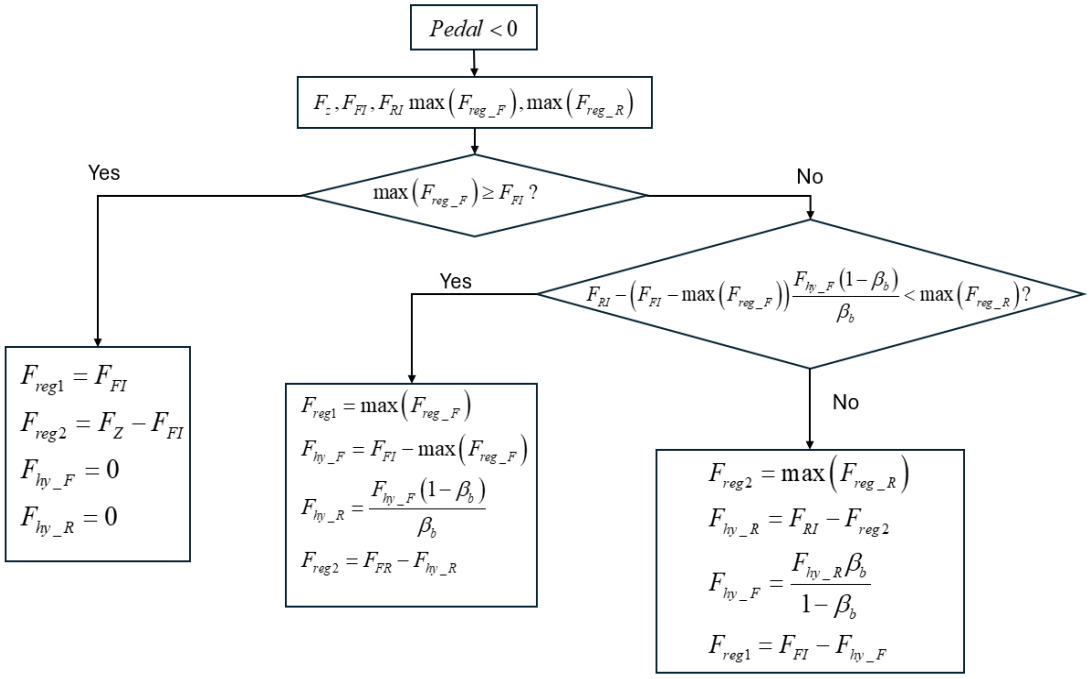

Fig. 4. Control algorithm logic of braking force distribution between front axle and rear axle at pedal under 0

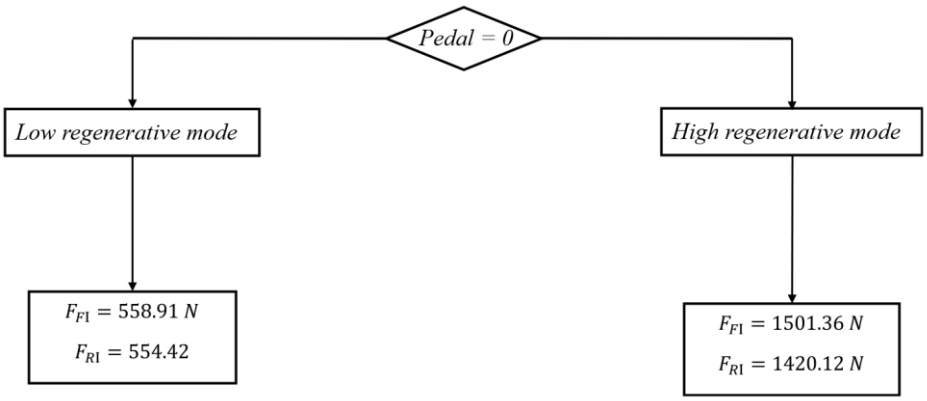

Fig. 5. Control algorithm logic of braking force distribution between front axle and rear axle at pedal equal 0

In the first case, pedal signal < 0: the maximum regenerative braking force of the front and rear motor are written as $\max(F_{reg\_F})$ and $\max(F_{reg\_R})$, respectively, are determined by the maximum regenerative capacity of the motor.

If $\max(F_{reg\_F}) \geq F_{FI}$, $\max(F_{reg\_F})$ can meet F_{FI}. So, the electric motor braking force and hydraulic braking force of the front axle is given as [5]:

$$F_{reg1} = F_{FI} \quad (5)$$

$$F_{hy\_F} = 0 \quad (6)$$

For the 4WD EV, the braking force required by the rear wheel is smaller than the braking force required by the front wheel in braking $F_{FI} > F_{RI}$. ~~Because~~ the front and rear motors of the EV are the same, $\max(F_{reg\_R})$ can also meet F_{RI} – the theoretical braking force of the rear axle. Therefore, the electric motor braking force and hydraulic braking force of the rear axle is expressed as:

$$F_{reg2} = F_{RI} = F_z - F_{FI} \quad (7)$$

$$F_{hy\_R} = 0 \quad (8)$$

where F_{RI} is the theoretical braking force of the rear axle.

If $\max(F_{reg\_F})$ is less than F_{FI}, the hydraulic braking force of front axle are given as:

$$F_{hy\_F} = F_{FI} - max(F_{reg\_F}) \quad (9)$$

The hydraulic braking force of front axle can be obtained:

$$F_{hy\_R} = F_{hy\_F}(1-\beta_b)/\beta_b \quad (10)$$

where β_b represents the hydraulic braking force distribution relationship of the front and rear axles, and it is defined as:

$$\beta_b = F_{hy\_F}/(F_{hy\_F} + F_{hy\_R}) \quad (11)$$

The distribution of hydraulic braking force between the front and rear wheels follows a fixed ratio, denoted β_b. For reference to the vehicle's mechanical braking system, this coefficient is 0.692. Under these conditions, two scenarios are analyzed as follows:

(1) If $\max(F_{reg\_F}) + F_{hy\_R} \geq F_{RI}$, the electric motor braking force of the rear axle can be obtained:

$$F_{reg2} = F_{RI} - F_{hy\_R} \quad (12)$$

(2) If $\max(F_{reg\_F}) + F_{hy\_R} \leq F_{RI}$, rear wheels are not locked. The electric motor braking force of the rear axle is defined as:

$$F_{reg2} = max(F_{reg\_R}) \quad (13)$$

According to curve I, the hydraulic braking force of the rear axle can be increased as:

$$F_{hy\_R} = F_{RI} - max(F_{reg\_R}) \quad (14)$$

The hydraulic braking force of the front axle is updated as:

$$F_{hy\_F} = \frac{F_{reg\_R}.\beta_b}{1-\beta_b} \quad (15)$$

The electric motor braking force of the front axle is defined as:

$$F_{reg1} = F_{FI} - F_{hy\_F} \quad (16)$$

The second case, pedal signal = 0: When the driver releases the accelerator pedal without engaging the brake pedal, allowing the vehicle to coast freely, the electric vehicle (EV) activates its regenerative braking system. This system generates braking torque, gradually decelerating the vehicle and ultimately bringing it to a complete stop.

The study examines two regenerative braking modes: Low and High. Utilizing Curve I, the optimal braking force distribution between the front and rear axles is determined for both modes when the motor operates within the constant torque region ($\omega_{motor} < 628.32$ rad/s).

Through simulation model analysis, the required front axle braking force F_{FI} is determined to be 558.91N (equivalent to 8% of the motor's regenerative capacity when operating in the constant torque region), applied to the front wheels. The proposed control strategy in the low regenerative mode achieves a braking acceleration of 0.5 m/s².

In the high-regeneration mode, a similar simulation analysis is conducted for a braking acceleration of 1 m/s². The braking force F_{FI} applied to the front axle is determined to be 1501.36N (equivalent to 21% of the motor's regenerative capacity when operating in the constant torque region).

Fig. 6. Two regenerative braking modes of VinFast VF8

According to the braking force distribution strategy above, the controller model of the braking energy recovery strategy based on curve I is simulated.

2.3. Evaluation methods of the All-wheel-Drive Electric Vehicle Model

2.3.1. Based on using WLTP

The WLTP (Worldwide Harmonized Light Vehicles Test Procedure) cycle is divided into four segments, each corresponding to a different speed

range: low, medium, high, and extra high. Throughout each segment, the vehicle undergoes a sequence of driving actions, such as stopping, braking, and accelerating. The test is conducted multiple times, beginning with a fully charged battery and continuing until the battery is completely depleted [10]. The objective of using WLTP is to compare the vehicle's driving range in simulation with the manufacturer's stated specifications.

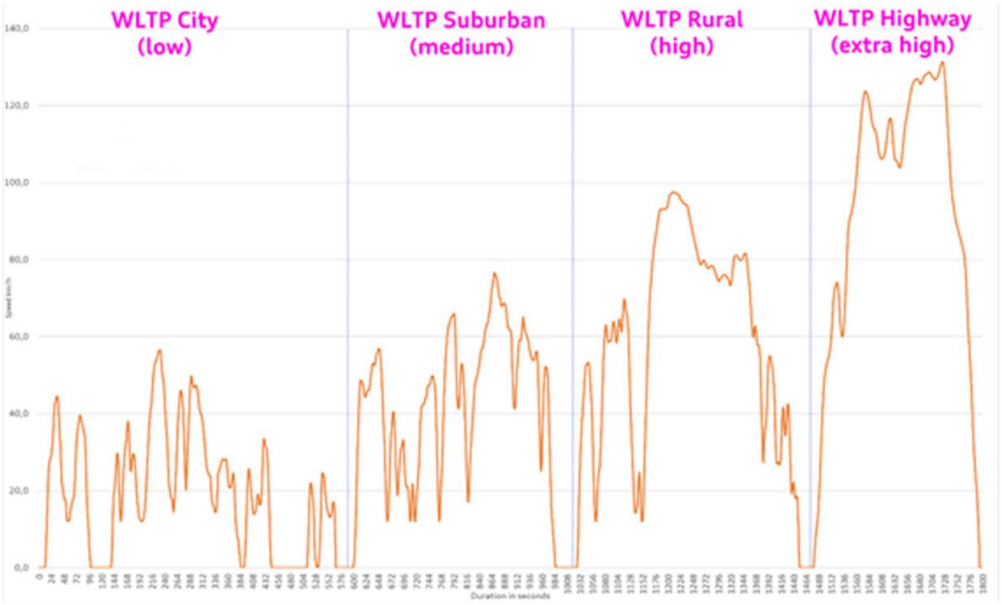

Fig. 7. Worldwide harmonized Light – duty vehicle Test Cycles – Class 3b

2.3.2. Experiment under real-world conditions

The purpose of this experiment is to evaluate the performance of reference vehicles by measuring longitudinal velocity, longitudinal acceleration, and braking distance when the driver does not press the brake pedal.

The experiment utilizes the VinFast VF8 – ECO model as the test vehicle, along with an S – Motion sensor to record dynamic parameters in driving dynamics tests. Additionally, a DTI – Logger data collector is used to gather experimental data and transmit it to a computer for analysis.

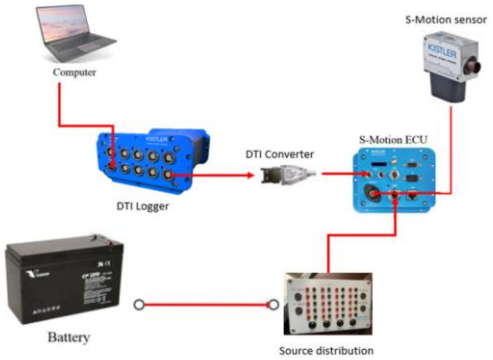

Fig. 8. Connection diagram

Fig. 9. The installation of S-Motion sensor

The test is conducted on a straight, dry asphalt road measuring approximately 1000 meters in length, with an adhesion coefficient of 0.8. The road is relatively flat, ensuring suitable conditions for the experiment. The following are the procedures for the experiment.

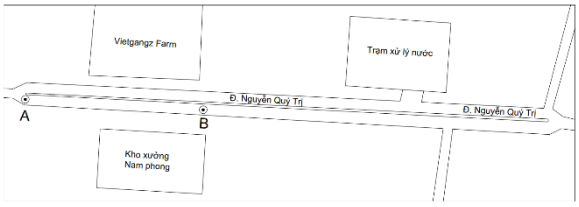

Fig. 10. The actual road

The experiment will be conducted in five steps as follows:

Step 1: The vehicle starts from point A and accelerates to point B (60 km/h). The data collector, seated in the passenger seat, will monitor the sensor parameters received from the vehicle to ensure that the connection is functioning properly.

Step 2: The vehicle reaches the designated position B at an approximate speed of 60 km/h. The vehicle speed is observed via the dashboard or through the speed parameters displayed on the monitoring screen.

Step 3: When the vehicle reaches the target speed at point B, the driver releases the accelerator pedal, and the regenerative braking system is activated in both low and high-regeneration modes. The vehicle will decelerate over different distances. The S-Motion sensor will capture the data and transmit signals to the ECU, which then sends the data to the computer for processing.

Step 4: Once the vehicle slows down to approximately 10-20 km/h, the software will receive the signal, and the data recording process will automatically stop.

Step 5: The results and data obtained during the experiment will be reviewed. The data collected will be analyzed, and all equipment and sensors will be checked. The process will then be repeated for subsequent test iterations.

3. Result and Discussion

3.1. Validation of the Electric Vehicle Model based on the WLTP Driving Cycle

Table 2 compares the driving range of the electric vehicle in the WLTP driving cycle under two regeneration modes: LOW and HIGH. The results show low errors in all cases (below 5%), confirming that the model is reliable enough to further evaluate the vehicle's dynamic parameters under real-world experimental conditions.

Table 2. The comparison of the model with the manufacturer's announcement

Regeneration Mode	Simulated driving range (km)	Driving range (provided by VinFast) (km)	Driving range error between simulation and Manufacturer's Information (%)
Low	481	460	4.57
High	535	510	4.90
Different ratios between regenerative modes	11.23%	10.87%	

3.2. Validation of the Electric Vehicle Model based on Dynamic Parameters

The experimental results for the test scenario described in Section 2.3.2 are presented for two modes: the LOW regeneration mode, illustrated in Fig. 3.1, and the HIGH regeneration mode, shown in Fig. 3.2. Experimental and simulation results confirm the high accuracy of the specific software, with velocity, acceleration, and braking distance closely matching experimental data. In the first scenario, MAE for velocity is 0.0008, and RMSE is 0.07 m/s, whereas in the second scenario, the MAE is slightly higher at 0.0022 m/s, with an RMSE of 0.11m/s. The braking distance simulation also aligns well with the experimental results, with RMSE values of 1.86 m and 1.3 m, respectively. The acceleration profiles exhibit a high correlation between simulation and experimental data, with negligible errors (RMSE under 0.09 m/s^2 and MAE close to 0). Although minor discrepancies exist, particularly in braking distance, these deviations remain within acceptable limits.

The overall results confirm that the AWD electric vehicle model accurately replicates real-world braking dynamics. With further parameter tuning, the model can be refined to enhance its precision.

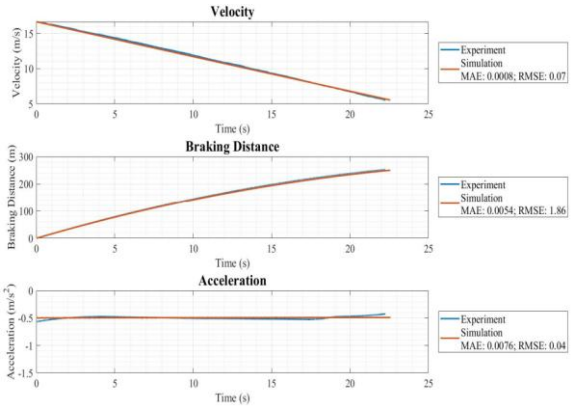

Fig. 11. Low-regenerative mode (60 km/h)

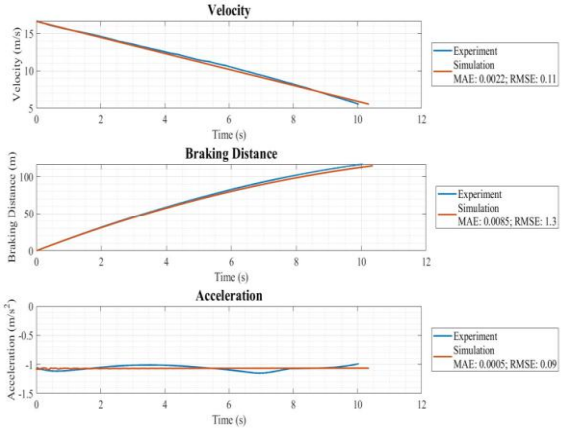

Fig. 12. High-regeneration mode (at 60 km/h)

3.3. Evaluation of Regenerative Capability across Different Driving Cycles in Vietnam

Survey regenerative energy on three actual driving cycles in Vietnam, including highway cycle, rush, and non-rush hours. These cycles are the results of surveys when running vehicle tests in Vietnam. Characteristic parameters and information of the cycles are shown in Table 3.

Table 3. Characteristic parameters and information of driving cycles

Cycle Driving	Highway	Non-rush hours	Rush hours
Distance (km)	73.61	8.54	14.41
Time (s)	2486	2059	5661
Average velocity (m/s)	29.62	4.15	4.20
Average velocity squared root (m/s)	29.94	5.42	4.01

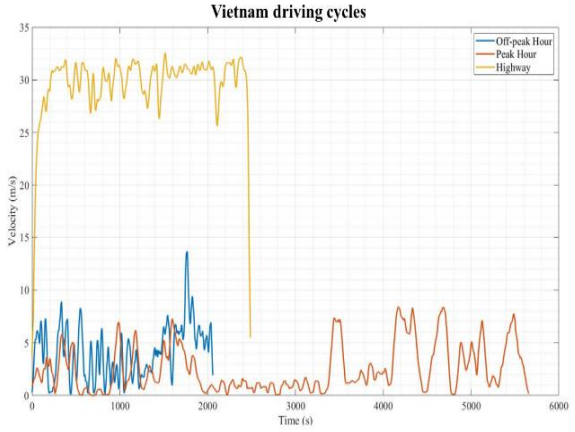

Fig. 13. Driving cycles

~~Below~~ Fig. 14 is a graph simulating the regenerative energy results in driving cycles in Vietnam with two regenerative braking modes: Low and High.

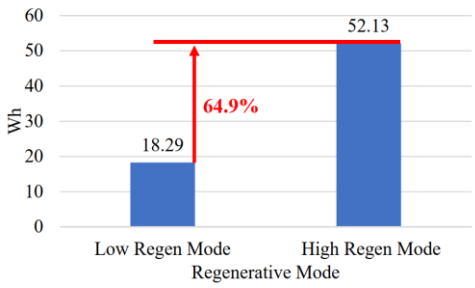

Fig. 14. Regenerative energy in non-rush hours driving cycle in Vietnam

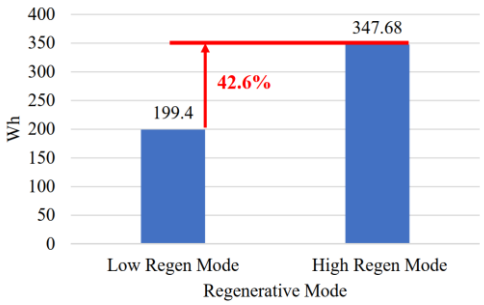

Fig. 15. Regenerative energy in rush hours driving cycle in Vietnam

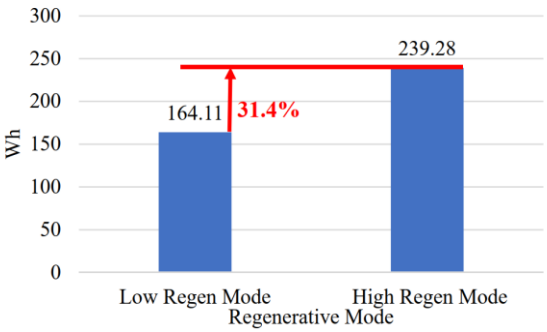

Fig. 16. Regenerative energy in the highway driving cycle in Vietnam

Table 4. Regenerative energy per 100 km for different regeneration modes in various driving cycles

Regenerative mode	Low (kWh/100km)	High (kWh/100km)
Non-rush hours	2.335	4.071
Rush hours	0.127	0.362
Highway	0.223	0.325

Based on the simulation results in Simulink, several key insights can be drawn regarding regenerative energy recovery efficiency under different traffic conditions in Vietnam. The high-regeneration mode consistently achieves better energy recovery performance than the low regeneration mode. However, the difference in efficiency between the two modes depends significantly on specific traffic conditions. In both LOW and HIGH regeneration modes, the total travel distance is greater during periods of low traffic density than during high traffic density. However, regenerative energy per 100 km is higher during non-peak hours compared to peak hours. This can be attributed to low travel speeds and the frequent stop-and-go traffic conditions during peak hours, where the continuous use of braking reduces energy recovery efficiency in both LOW and HIGH regeneration modes. Under highway driving conditions, regenerative braking efficiency decreases

significantly due to higher vehicle speeds and fewer braking events, limiting opportunities for energy recovery.

This analysis highlights the importance of optimizing the regenerative braking algorithm based on specific traffic conditions to maximize energy efficiency, particularly in dynamic urban environments.

4. Conclusion

This study provides an in-depth analysis of regenerative braking efficiency under various traffic conditions using specific simulation software. The results highlight that regenerative braking performance is significantly influenced by traffic density, with the highest energy recovery observed in urban stop-and-go conditions and the lowest in highway driving due to fewer braking events. The comparison between low and high-regeneration braking modes confirms that while High Regen Mode consistently yields superior energy recovery, the efficiency gap between the two modes depends on driving patterns. The key contribution of this research lies in its systematic evaluation of regenerative braking across different driving cycles, offering insights into optimizing vehicle energy management strategies. These findings are particularly relevant for urban transportation planning and electric vehicle control systems, where maximizing energy recovery can enhance overall efficiency and sustainability.

Furthermore, future research will focus on developing a real-world vehicle model, incorporating measurement, analysis, and evaluation of regenerative energy recovery performance under Vietnam's specific driving cycle conditions. Additionally, upcoming studies will assess driving experience and safety aspects during braking operations, particularly the integration of regenerative braking with the ABS system to optimize braking performance and ensure operational safety.

Acknowledgment

Funding: This research is funded by the Hanoi University of Science and Technology under project number T2025-PC-023.

References

[1] G. Sandrini, D. Chinamo, and M. Garcola, Regenerative braking logic that maximizes energy recovery ensuring the vehicle stability, in Energies, vol. 15, no. 16, Aug. 2022, Art. no. 5846. https://doi.org/10.3390/en15165846

[2] J. Valladolid, M. Calle, and A. Guiracocha, Ingenius - Revista de Ciencia y Tecnología, Analysis of regenerative braking efficiency in an electric vehicle through experimental tests, no. 29, pp. 24–31, Jan. 2023. https://doi.org/10.17163/ings.n29.2023.02.

[3] M. H. Hwang, G. S. Lee, E. Kim, H. W. Kim, S. Yoon, T. Talluri, and H. R. Cha, Applied sciences, Regenerative braking control strategy based on AI algorithm to improve driving comfort of autonomous vehicles, in Applied Sciences, vol. 13, no. 2, Jan. 2023. https://doi.org/10.3390/app13020946.

[4] S. Li, B. Yu, X. Feng, Science Progress, Research on braking energy recovery strategy of electric vehicle based on ECE regulation and I curve, in Science Progress, vol. 103, no. 1, pp. 1–17, Jan. 2020. https://doi.org/10.1177/0036850419877762.

[5] Z. Ma, D. Sun, Energy recovery strategy based on ideal braking force distribution for regenerative braking system of a four-wheel drive electric vehicle, IEEE Access, vol. 8, pp. 136234–136242, Jul. 2020.

[6] V. N. Le, The power train modelling of an all-wheel-drive electric vehicle, *Автотракторостроение и автомобильный транспорт : сборник научных трудов* , vol. 1, pp. 50–58, 2024, Minsk, Belarus: Belarusian National Technical University, 2024.

[7] V. N. Le, H. P. Dam, and V. P. Dinh, A longitudinal dynamic model of an all-wheel-drive vehicle, *Автотракторостроение и автомобильный транспорт: сборник научных трудов*, vol. 1, pp. 30–37, Minsk, Belarus: Belarusian National Technical University, 2024.

[8] E. Yurdaer, T. Kocakulak, Comparison of energy consumption of different electric vehicle power systems using fuzzy logic-based regenerative braking, Engineering Perspective, vol. 1, no. 1, pp. 11–21, Mar. 2021. http://dx.doi.org/10.29228/sciperspective.47590

[9] VinFast, [Online] Available: https://vinfastauto.us/vehicles/vf-8, Accessed on: Feb 15, 2025.

[10] WLTPFACTS.EU, WHAT IS WLTP AND HOW DOES IT WORK?, [Online]. Available: https://www.wltpfacts.eu/what-is-wltp-how-will-itwork/, Accessed on: Jan 9, 2025.